JAST
Journal of Aerospace Science and Technology

Pages: 26-36/ Vol. 15/ No. 1 / Winter- Spring 2022

Journal of Aerospace Science and Technology

www:jast.ias.ir

Scientific- Research Article

Designing an Ultrasonic Wind Tunnel with a Steam Ejector System of Combined Cycle Power Plants

Hossein Shadmehr[1]*, **Sajad Ghasemloo**[2], **Hamid Parhizkar**[3]
1-2-3- Department of Aerospace Engineering, Malek Ashtar, Tehran, Iran

ABSTRACT

The idea of constructing an ultrasonic wind tunnel using a steam ejector and superheated steam flow in combined cycle power plants is investigated through computational fluid dynamics. Using a small portion of the plant's generated steam as a high-pressure source in the steam ejector can create an ultrasonic airflow in the test chamber. The applied numerical model is a viscous compressible flow that has been modeled with the SST K-Omega turbulence model. All calculations are performed in Ansys Fluent commercial software. After validating the numerical process, different geometries have been proposed to achieve the ultrasonic secondary flow, and each structure has been numerically examined separately in a range of operating conditions. Based on the previous findings, a trial and error method, and experimenting with several different structures, a suitable structure for obtaining the ultrasonic test chamber has been achieved. This structure has been parametrically studied in different functional conditions. It is shown that the proposed structure can generate secondary ultrasonic flow in an acceptable range of pressure and flow of superheated steam in the power plant. This structure has been presented for the first time in the literature, and such a structure has not been suggested in any of the previous works. Therefore, the achievement of the secondary ultrasonic flow is the main innovation of this research.

***Keywords**: wind tunnel; Steam ejector; Combined Cycle Power Plant; Computational Fluid Dynamics*

Introduction

The project's primary purpose is to change the design of the steam ejector using the numerical method so that high-speed wind tunnels can be obtained in addition to the combined cycle power plants. This is achieved using the steam pressure supplied in the power plant. In general, high-speed wind tunnels are those in which the flow reaches the flow's velocity (Mach number) in the compressible range. Therefore, a wind tunnel with a sonic or supersonic range is considered in this research.

A wind tunnel is a tool for monitoring the flow in the laboratory. The importance of wind tunnels is due to the high cost of testing the model in actual dimensions and the number of risks in flight testing. Wind tunnels can be classified according to their type of operation, design, and speed. The wind tunnel presented in this research is of high-speed open circuit type in the subsonic to the supersonic range. The main challenge in designing

1 Msc (Corresponding Author) **Email: *** shadmehr.h@gmail.com
2 Assoicate Professor
3 Assoicate Professor

DOI : 10.22034/jast.2022.297517.1087
Submit: 31.07.2021/ Accepted: 02.02.2022
Print ISSN:1735-2134 Online ISSN: 2345-3648

a high-speed wind tunnel is to provide the energy needed to increase the flow rate. Most high-speed wind tunnels operate between a high-pressure and a low-pressure chamber. Accordingly, the high-pressure air stored in the high-pressure chamber is accelerated through a nozzle and transferred to the low-pressure one. In the middle of the flow path, there is a test chamber with the studied model, which is connected to the measuring instrument. Existing methods for constructing high-speed wind tunnels are costly. Moreover, high-speed wind tunnels, especially ultrasonic tunnels, operate for a very limited time, and a stability issue will be raised due to the rapid drop in the pressure of the high-pressure chamber. Some high-speed wind tunnels use a closed-loop design to increase the flow stability, which will cost much more than an open-loop design.

The present paper uses the idea of a power plant ejector system in a high-speed wind tunnel to provide a low-cost method for constructing and supplying the necessary energy for a high-speed wind tunnel. Superheated steam in combined cycle power plants is available at different pressure and temperature levels to move the steam turbine shaft. At the turbine inlet, the characteristics of this steam are up to 90 atmospheres and 530 degrees Celsius with a flow rate of 134 kg/s. Commonly, part of this steam (with a pressure of 15 atmospheres, 250 ° C, and a flow rate of less than 0.3 kg / s) is used to run steam turbines using an ejector. This steam is used in a system similar to the ejector to move air in a high-speed wind tunnel in the present study. This does not disrupt the operation and efficiency of the power plant.

There are generally two types of mixing for ultrasonic ejectors, including constant-pressure mixing (CPM) and constant-area mixing (CAM). The difference between the two designs is in choosing ultrasonic mixing in a convergent nozzle (pressure-constant) or in a channel (constant-area mixing).

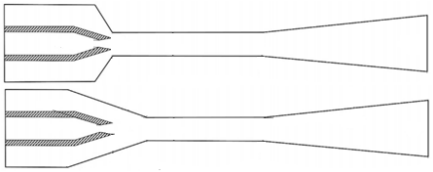

Figure 1. Two types of ejectors with respect to mixing type, constant-area ejector (above), constant-pressure ejector (below)

So far, many models of ejectors have been introduced. Most of these models seek to build constant-pressure ejectors and constant-pressure and constant-area mixing designs. By examining the effect of back pressure and inlet temperature on a constant-area steam ejector, Hanafi et al. [1] showed the dependence of operating parameters and entertainment ratio on the inlet temperature of steam. This paper presented a specific geometry for the ejector that can be reconstructed and used as a validation reference. At first, mathematical modeling shows the dependence of operating parameters on functional parameters (temperature and pressure) and design parameters (dimensions and diameter of the throat). Then steam was assumed as the ideal gas based on the previous research, and modeling was performed with the Ansys Fluent software. Finally, the entertainment ratio is calculated as a functional parameter of the ejector at different back pressures and inlet pressures. This number was also calculated at different inlet temperatures, and it was concluded that with increasing the inlet steam temperature, the entertainment ratio also increases.

Ahmadabadi et al. [2] tried to create the required Mach number in the test chamber by blowing high-speed air in a certain wind tunnel section using the ejector system. The designed ejector system is a three-stage and concentric ejector modeled step by step, assuming that the stagnation pressure is constant. The comparison demonstrated that the modeling results was very close to the experimental data of the wind tunnel test. Bazazzadeh et al. [3] have tried to control the Mach number in the test chamber of an ultrasonic blowing wind tunnel by controlling the pressure in the relaxation chamber by one or more flow control valves. Hence, a blowing ultrasonic wind tunnel was simulated in MATLAB software. Then, by creating a proportional-integral controller, the opening rate of the flow control valve was adjusted, and as a result, the pressure and the flow velocities in the test chamber were controlled. The control function was optimized using genetic algorithms, which led to the fast running of wind tunnels and longer wind tunnel execution time. Doulabi et al. [4] have also presented a diffuser design process with a fixed geometry that can maintain a flow with a Mach of 5, 6, and 7 inside the test chamber with the lowest pressure ratio for the tunnel. The diffuser structure is similar to a single-stage ejector, and a test chamber is installed after the convergent-divergent nozzle. By changing the throat diameter, diffuser length, length to diameter ratio, and pressure ratio,

velocity in the wind tunnel was optimized. Keenan et al. [5, 6] proposed two different design methods for the ejector, known as the constant-area mixing (CAM) and the constant-pressure mixing (CPM). The concept of a constant-area mixing, first introduced in 1942 [5], proposes an area with a fixed cross-section for the entire mixing chamber, where the primary nozzle outlet is located at the beginning of the chamber and is suitable for flows with high mass rates. The concept of constant-pressure mixing was introduced in 1950. This concept, used in most ejectors today, has a better performance than constant-area ejectors [7]. The geometry of the constant-pressure ejector consists of a variable cross-section prior to the fixed cross-sectional area. In references [8] and [9], constant-pressure and constant-area mixing designs have been compared for several boilers and different steam temperatures with experimental and numerical methods. Accordingly, it has been shown that CAM design has a higher entertainment ratio but lower density than CPM design [10, 11]. Wang et al. [12] and Sriveerakul [13] separately showed that the increase in ω depends on the increase in φ until it reaches a certain value. However, the critical back pressure decreases with the increase of these quantities. Varga et al. [14] conducted research based on these concepts, which showed that increasing the throat diameter in the mixing chamber will increase ω. Jia et al. [15] experimentally evaluated the effects of operating conditions such as primary flow pressure on the performance of a system of ejectors with constant and variable area ratios. They showed that the effect of this factor on the performance of the ejector is highly dependent on the operating conditions. Yan et al. [16] demonstrated the existence of an optimal value for φ under stable operating conditions by testing an R134a ejector. The results of CFD in the research carried out by Mohamed et al. [17] prove that increasing φ will increase ω and decrease critical back pressure. Pianthong et al. [18] studied a steam ejector and showed that CFD could model the ejector in constant conditions and show the device's performance well. These results were accompanied by validation of numerical results with pressure distribution and overall experimental performance. Sriveerakul et al. [19] described the mixing process with graphical diagrams and numerical simulation. Their results proved the existence of effective areas in the mixing chamber, which was proposed by Huang et al. [20]. Also, the existence of two series of oblique shocks in the primary nozzle output and diffuser input has been identified in this research. The CFD results also discuss the phenomena of flow mixing, jet center effect, and oblique shocks. Ruangtrakoon et al. [21] investigated the effects of primary nozzle geometry, in-stream structure, parameter distribution, and performance. It was found that the location of oblique shocks and the angle of the primary flow at the outlet of the nozzle can play a significant role, depending on whether the primary flow jet is dilated or extended. Riffat et al. [22] used CFD to evaluate the performance of the ejector under the conditions of using heat pumps and different nozzles. Also, the location of the nozzle relative to the mixing chamber has been investigated in this study. The effects of various fluids have also been investigated separately, including ammonia, R134a, and propane as fluids. Using CFD simulations and experiments, Zhang et al. [23] investigated the design of an R236fa ejector and an NXP with a variable nozzle output angle to assess the best performance under uniform input conditions and a range of output pressures. Zhang et al. [23] investigated the effects of convergent-divergent nozzle angle, throat length, and wall roughness on the overall performance of the ejector.

This research presented a practical design for a high-speed wind tunnel in the range of subsonic to supersonic using the ejector system. In this design, a suitable aerodynamic design will create a high-velocity flow in the secondary flow passage of the ejector. Moreover, installing a test chamber as a wind tunnel is predicted in some areas of this passage. The resulting wind tunnel can operate in the range of ultrasonic to ultrasonic in stable conditions. It does not have any rotating elements and compressors and does not need a high-pressure and low-pressure chamber. It is fed directly from the open atmosphere. In other words, all the energy needed to move the air comes from the high-pressure steam of the power plant. Compared to all flow high-speed wind tunnels, the ejector wind tunnel provides long-term uniform flow at supersonic speeds without a rotating element. In this tunnel, the high-pressure steam wind of the power plant, which is usually wasted, is considered the flow stimulator. In some previous inventions, ejectors in tunnel winds have been predicted to improve their performance. However, in the present study, the aerodynamic design method of wind tunnels is based on ejectors and does not

require any power source independent of the initial inlet steam of the ejector.

Figure 2 shows the wind tunnel in question. Superheated steam from the power plant operation enters the converging section of the primary flow nozzle (1) through a high-pressure steam transfer pipe. This initial airflow enters the mixing chamber (4) after passing through the throat of the primary nozzle (2) and the divergent part of the nozzle (3). The secondary channel starts from the input (5) of the convergent-divergent nozzle (6). After the convergent-divergent nozzle, the flow enters the test chamber (7). After the test chamber, a divergent channel (8) is installed to create the right angle, which is necessary for the stability of the flow. In other words, it acts as a diffuser. The two primary and secondary flows exit the wind tunnel outlet (10) after mixing in the mixing chamber through a divergent diffuser (9).

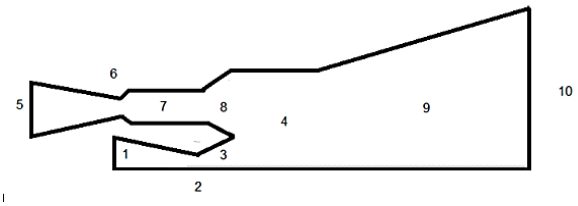

Figure 2. Ejector wind tunnel

Governing equations and numerical model

The Navier-Stokes equations (governing equations for viscous fluid) are used in the numerical model, assuming the fluid is compressible. The discrete equations in the final problem model are the Navier-Stokes equations in survival form. These equations are expressed in the form of matrices used in the computational code. They are shown in equations number one to three.

$$U_t + F(U)_x + G(U)_y + H(U)_z = Q \qquad (1)$$

$$U = \begin{bmatrix} \rho \\ \rho u \\ \rho v \\ \rho w \\ E \end{bmatrix}, \quad F = \begin{bmatrix} \rho u \\ \rho u^2 + p - \tau_{xx} \\ \rho uv - \tau_{xy} \\ \rho uw - \tau_{xz} \\ u(E+p) - (\bar{\bar{\tau}} \cdot \vec{v})_x - k\partial_x T \end{bmatrix},$$

$$G = \begin{bmatrix} \rho v \\ \rho uv - \tau_{yx} \\ \rho v^2 + p - \tau_{yy} \\ \rho vw - \tau_{yz} \\ v(E+p) - (\bar{\bar{\tau}} \cdot \vec{v})_y - k\partial_y T \end{bmatrix}, \quad H = \begin{bmatrix} \rho w \\ \rho uw - \tau_{zx} \\ \rho vw - \tau_{zy} \\ \rho w^2 + p - \tau_{zz} \\ w(E+p) - (\bar{\bar{\tau}} \cdot \vec{v})_z - k\partial_z T \end{bmatrix}, \qquad (2)$$

$$\tau_{ij} = \mu\left[\left(\frac{\partial v_j}{\partial x_i} + \frac{\partial v_i}{\partial x_j}\right) - \frac{2}{3}(\vec{\nabla} \cdot \vec{v})\delta_{ij}\right]$$

$$\mathrm{E} = \rho\left(\tfrac{1}{2}\boldsymbol{V}^2 + e\right) \qquad (3)$$

In these equations, the expression $\bar{\bar{\tau}}$ is the shear stress tensor and $\vec{v}$ is the fluid velocity vector. The expression $\frac{1}{2}\boldsymbol{V}^2$ is defined by Equation (3). The relationship between pressure (p) and internal energy (e) is considered according to formula (3), which expresses the thermodynamic properties of the ideal gas. The non-slip wall boundary condition represents areas bounded by solid surfaces. At this boundary, the condition of non-slip is considered for shear stress. Moreover, zero roughness height and a roughness constant of 0.5 are applied to determine the roughness of the walls. In cases where the geometry has an axis of symmetry, the axial symmetry boundary condition is used. Conventional ejectors usually have axial symmetry. Hence, two-dimensional modeling can be applied using the axial symmetry condition on the symmetry axis. In this boundary condition, the velocity and pressure, and the turbulence characteristics of the inlet flow are determined. Also, the velocity angle is determined relative to the boundary wall or the absolute velocity angle. The velocity at the boundaries is determined by considering the Reynolds number of the flow. The output boundary condition in the ultrasonic flow is particularly critical. In numerical solution, the ultrasonic flow is not transmitted in the reverse direction by the upwind method, and the output boundary condition may not affect the field. In a convergent-divergent nozzle, the ultrasonic output will be maintained if the initial conditions are given so that the ultrasonic flow occurs at the output. This may lead to solution instability (divergence or oscillating solution) or non-physical response. In order to control the condition of the output boundary during the solution, it is crucial to select the appropriate initial conditions. The total length of the ejector is 3 meters (Figure 3), and its cross-section is composed of smooth lines that make it possible to reconstruct the geometry. This ejector revolves around a symmetrical central axis, which justifies its two-dimensional simulation of axial symmetry. It has been stated in many references that two-dimensional symmetric axial simulation and three-dimensional ejector simulation will have the same results. Figure 4 shows the pressure distribution in the centerline of the ejector and on its wall based on the reference [1].

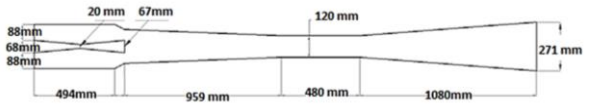

Figure 3. Ejector geometry studied in the reference [1]

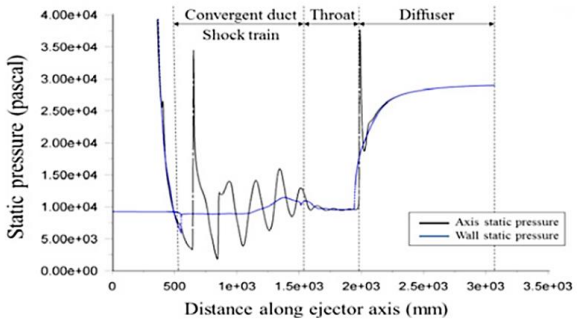

Figure 4. Pressure distribution in the center line and on the nozzle wall of the mixing section [1]

Numerical solution conditions and boundary conditions used in the model in FLUENT software are presented in Table 1. In the air inlet (secondary inlet), steam is used with low pressure and temperature. Due to its proximity of density to the air and the selection of the ideal gas model, it had a very close behavior with air, and the model was single-phase.

Table 1. Numerical solution conditions carried out in the stage of checking the independence of the network

Solution characteristics	Selected setting
Geometric model	2d-Axisymetric
Type of solution	Density-based, steady, Implicit
Boundary condition	Pressure outlet-Pressure inlet
Fluid	Steam
Numerical method	2nd order-Upwind
Numerical flux	Roe-FDS
Courant number	0.5
Convergence criterion	Reducing the remainder by three times (one thousandth of the initial value) and fixing the mean Mach number in the solution field

Networking and independence from the network

This section investigates the effect of the numerical model on networks with different densities. The process of selecting networks is based on halving each network's cell size, except for the network with 26,000-cell. This network is generated as a control for a network with 16,000 cells, which means that the trend of change near the independent network is also known. All calculations of this section have been performed with an initial static pressure of 6.7 bar, the temperature of 180 ° C, secondary pressure of 0.094 bar, a secondary temperature of 45 ° C, the static pressure of 0.28 bar, and a temperature of 115 ° C. Other specifications are in accordance with the reference [1].

Network No. 1 is obtained from the initial division of the field so that there are only two rows of cells inside the convergent-divergent nozzle of the primary flow. Contrary to expectations, this network has also provided acceptable results, especially in the entertainment ratio of primary and secondary flow. Dense networks are also produced by halving the cell dimensions of this network. All networks have the same density ratios. Network 5 has been investigated to evaluate the effects of minor changes in the dimensions of the independent network (a network with 16,000 cells). Images of the networks generated during the network independence test are presented in Figure 5.

Table 2. Specifications of cell dimensions in networks produced in the process of network independence

Network number	cell dimension (mm)	Two-dimensional cell number
1	5	187
2	2	1076
3	1	4298
4	0.5	16625
5	0.4	26153
6	0.2	104567

Figure 4 compares Mach number contours in different networks. Most Mach number variations are observed in the output range of the primary nozzle and the mixing chamber.

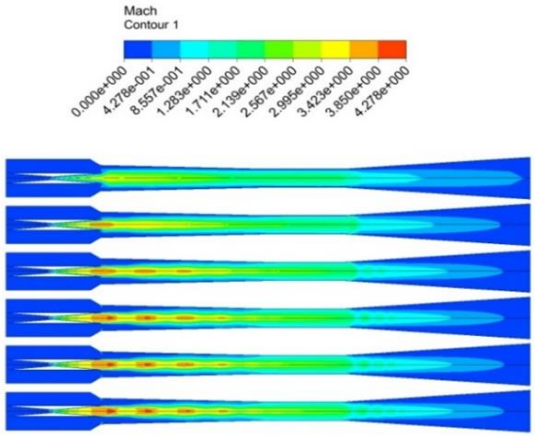

Figure 5. Mach number contours in the ejector

Table 3 presents the operating parameters, which are the mass rate at the high-pressure inlet, the mass rate at the low-pressure inlet, and the ratio of these two rates. It can be seen that this rate does not differ significantly between different networks. An initial network with two rows of cells will predict the entertainment ratio with less than 10% error.

The numbers in Table 3 are shown in Figure 6 in the form of a graph. In these diagrams, the slope of changes in networks numbers 3 to 6 can be ignored and is close to zero.

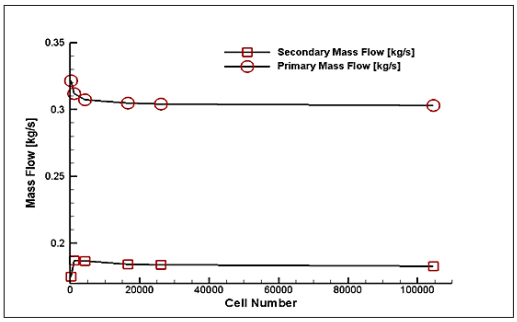

Figure 6. Effects of increasing the number of network cells on the primary and secondary mass rates

Table 3. Ejector performance parameters on networks with different densities

Network number	Initial mass flow rate]kg s^-1[	Secondary mass flow rate]kg s^-1[	Mass ratio of secondary flow to flow
1	0.32	0.17	0.54
2	0.31	0.18	0.59
3	0.3	0.18	0.6
4	0.3	0.18	0.6
5	0.3	0.18	0.6
6	0.3	0.18	0.6

Validation

The results obtained in the optimal network are compared with the results presented in the reference [1] to assess the validity of the numerical solution. Figure 7 shows the Mach number contours in the entire solution field compared to the contours provided in the numerical reference. Contour comparison is a qualitative comparison and only shows the similarity of the flow structure in the two numerical solutions.

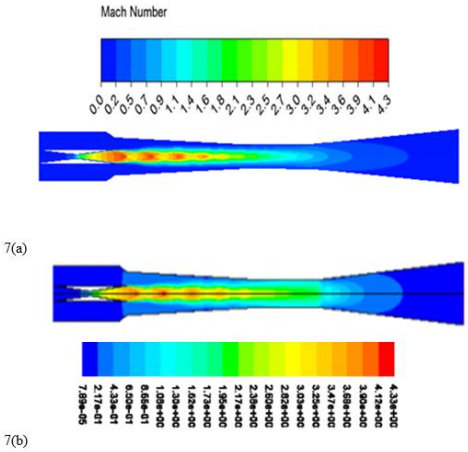

Figure 7. Mach number contours in the ejector. The numerical solution in a back pressure of 0.28 atmospheres (Figure 7a). Results of reference numerical solution at different pressures (Figure 7b) [1]

In order to quantify the validity of the numerical solution, the ratio of the mass rate of the secondary flow to the reference's primary flow [1] is compared with the numerical response. Table 4 presents these values with the error percentage. The error rate is less than 1% and is almost zero. This comparison shows that numerical solution is very accurate in predicting operating and overall parameters. This perfect agreement is due to the proximity of the flow to the ideal flow and the insignificance of the viscous phenomena in the flow.

Table 4. Comparison of numerical and experimental estimates of the ratio of secondary to initial mass in the ejector

Network number	The ratio of the mass of the secondary flow to the primary flow	Error percentage
Optimal network response	0.604	۰.۱٪
Experimental reference	0.605	۰

General design of ejector-wind tunnel system

In order to achieve a practical design, the wind tunnel system must first be designed next to the ejector based on the quasi-one-dimensional isentropic flow equations. Assuming the flow is isotropic and quasi-one-dimensional, the cross-sectional area of the primary and secondary nozzles can be determined. The throat surface of the secondary nozzle is highly dependent on the actual performance of the primary nozzle. After mixing, the flow will pass through a convergent-divergent nozzle, which can be supersonic or ultrasonic. Generally, the system indicates a nonlinear behavior. Another critical factor in designing the nozzle is the angle of the divergent part of the primary nozzle. This angle determines the distance between the primary ultrasonic flow and the wall and the pressure behind the secondary nozzle. The larger the angle, the more stable the flow in the secondary nozzle will be. However, at a constant-area ratio, increasing the divergent nozzle angle can cause the flow to suffocate due to the separation of the boundary layer. The main design of the ejector-wind tunnel system and its components are presented in Figure 8.

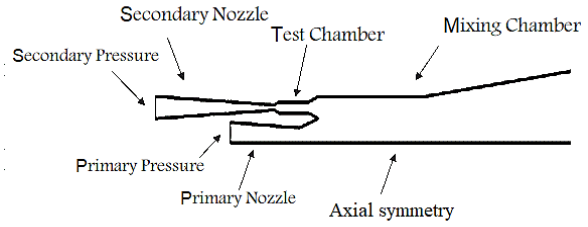

Figure 8. Proposed design for ultrasonic wind tunnel with ejector system

Figure 9 shows the pressure contour's best performance in creating a supersonic flow in a wind tunnel based on numerical simulation. This design is created using a CAM-designed ejector and a divergent nozzle installed after the test chamber. This design has the most stability against changes in inlet pressure and the primary nozzle geometry. Stability means achieving a constant flow over time. The obtained design is examined parametrically in two separate processes. The effects of primary gas pressure (high-pressure steam) and the secondary nozzle throat changes have been investigated on the flow characteristics in the test chamber and the flow in the whole system.

Investigating the effect of primary gas pressure

This section investigates the effect of primary gas pressure (high-pressure steam) on the flow characteristics in the wind tunnel test chamber and the whole system. Steam pressure can be supplied to the target power plant at 90 and 15 atmospheres. The inlet pressure will decrease with increasing system dimensions due to the use of steam at a pressure of 15 atmospheres, the loss of piping, and the reduction of pressure by increasing the cross-sectional area of the primary nozzle (in order to achieve a larger cross-sectional area in the test chamber). In this section, the effect of pressure reduction is investigated by keeping the dimensions constant, which is equivalent to increasing the device's dimensions. Table 5 presents the mass rate changes in the two primary and secondary nozzles and the ratio of these two mass rates to the increase in inlet pressure of the primary nozzle. By increasing the back pressure to more than seven atmospheres, there is no increase in the mass rate in the secondary nozzle and reaches its maximum value.

Table 5. Changes in mass rate and entertainment ratio with increasing primary nozzle inlet pressure

Primary nozzle inlet pressure [Bar]	Mass rate in the primary nozzle (m_1) [kg s^-1]	Mass rate at the secondary nozzle (m_2) [kg s^-1]	$\omega = \frac{m_1}{m_2}$
3	4.64	2.87	0.61
5	7.74	2.9	0.37
6	9.29	2.85	0.3
7	10.84	2.85	0.26
8	12.4	2.85	0.23
10	15.5	2.85	0.18
12	18.61	2.85	0.15

Figures 9 to 16 show temperature contours for inlet pressures of 12 atmospheres to a pressure of 3 atmospheres. It can be seen that at high pressures, the low-temperature zone is visible in the mixing chamber. As the inlet pressure decreases, the temperature of the mixing area and the wind tunnel test chamber increases, and the temperature at the outlet of the nozzle at the end of the system decreases. This phenomenon is created due to the decrease in shock power and pressure reduction in the output of the primary nozzle. The most important phenomenon in the whole system is the arc shock at the output of the primary nozzle. This

arc shock is accompanied by a sharp decrease in temperature and Mach number.

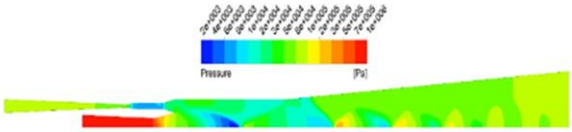

Figure 9. Pressure contour under primary pressure conditions p_1 = 12 Bar

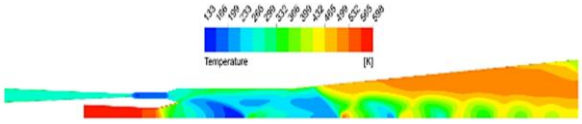

Figure 10. Temperature contour under primary pressure conditions p_1 = 12 Bar

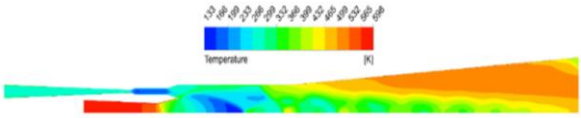

Figure 11. Temperature contour under primary pressure conditions p_1 = 10 Bar

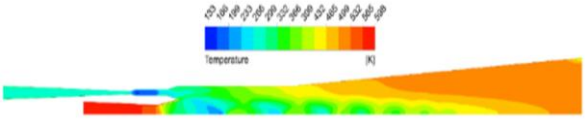

Figure 12. Temperature contour under primary pressure conditions p_1 = 8 Bar

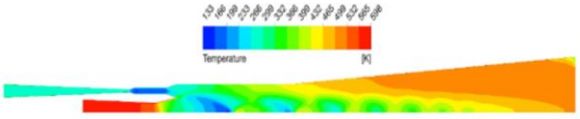

Figure 13. Temperature contour under primary pressure p_1 = 7 Bar

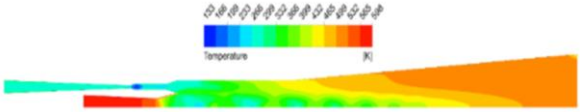

Figure 14. Temperature contour under primary pressure conditions p_1 = 6 Bar

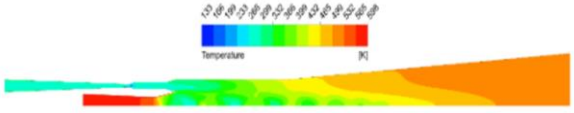

Figure 15. Temperature contour under primary pressure conditions p_1 = 5 Bar

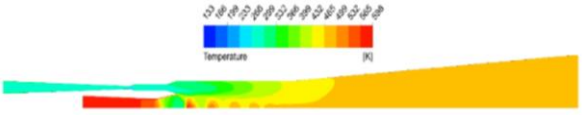

Figure 16. Temperature contour under primary pressure conditions p_1 = 3 Bar

A close-up of the mixing chamber in Figure 17 shows that at inlet pressures of less than 8 atmospheres, a shock forms at the outlet of the primary nozzle, which increases the pressure behind both nozzles and decreases system efficiency.

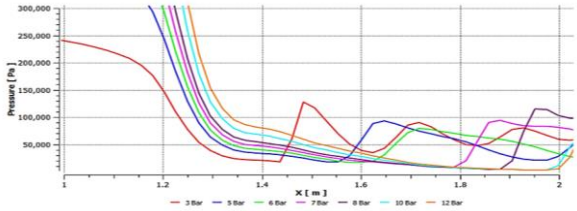

Figure 17. Pressure changes in the symmetry axis of the ejector and the mixing chamber in the mixing range

In the mixing chamber, a sudden decrease in Mach number and the shock approaching the output of the primary nozzle reduces the power of flow generation in the test chamber (secondary nozzle). In these diagrams, it can be seen that at pressures of 12 and 10 atmospheres, the flow in the test chamber is almost the constant Mach. However, it changes with decreasing in the flow pressure in the chamber. At pressures of less than 5 bar, the flow is entirely subsonic.

Effect of secondary nozzle size on performance and flow

This section investigates the effect of nozzle throat diameter changes on the performance of the wind tunnel system. In these three geometries, the ratio of the throat diameter to the test chamber diameter has different values. The geometries are compared in Figure 18, showing that the changes are minimal. The values of the throat diameter to test chamber diameter ratio are presented in Table 6. The simulations of this study were performed at an inlet pressure of 8 bar.

Table 6. Ratio of throat diameter to test chamber diameter

Geometry number	Ratio of throat diameter to test chamber diameter
1	0.44
2	0.53
3	0.66

Figure 19 shows the Mach number contours for three geometries with different throat diameters. As the throat diameter decreases, the Mach number in the test chamber increases. This

increase in Mach number causes changes in the flow in the mixing chamber. It can be seen that the expansion fan is more powerful at the output of the primary nozzle, which causes an arc shock in the mixing chamber, and an arc shock is formed at a higher Mach number.

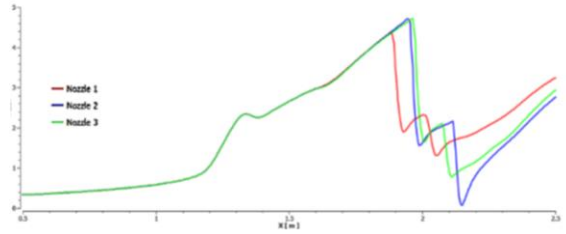

Figure 18. Mach number changes in the centerline of the primary nozzle for three different throats

Figure 18 shows the Mach number changes in the centerline of the primary nozzle (symmetry line of the two-dimensional model) for three different throat diameters. In nozzle No. 3, which has the smallest throat diameter, Mach number has the maximum value (green line). The smallest flow changes are observed in the mixing chamber in Geometry # 1 (red line). The effect of the secondary nozzle diameter on the flow in the mixing chamber is quite clear.

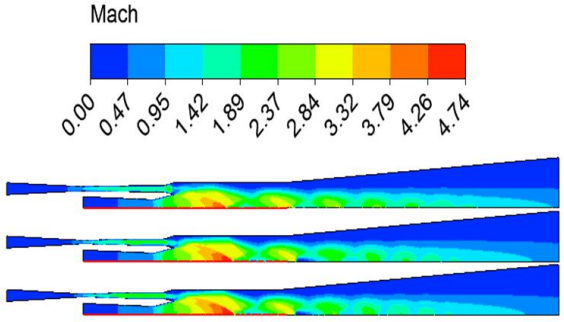

Figure 19. Mach number contours for geometries 1 to 3 from bottom to top

Conclusion

In this research, the design of a high-speed wind tunnel in the ultrasonic range was investigated using the power plant's ejector system and steam pressure. Numerical flow simulation in the ejector and wind tunnel was investigated using the numerical method in Ansys Fluent software. A sample supersonic ejector with variable cross-section was examined to measure the accuracy and validity of the numerical model. A good agreement was observed during validation between the present numerical results and the previous numerical and laboratory results. The final design selected from different evaluated designs included a convergent-divergent nozzle before the tunnel wind chamber and a CAM-designed ultrasonic ejector. This design stabilizes the flow in the mixing chamber. Stability means that the flow does not change over time and the shock location and the expansion fan are constant throughout the ejector. A wind tunnel designed with an ejector system with a primary pressure supply between 8 to 12 bar can produce ultrasonic flow in the range of 1.8 <M <2.3 depending on the supplied pressure and the design of the ejector wind tunnel system. The final design does not require a high-pressure air chamber and a low-pressure chamber to discharge. Therefore, it operates between two atmospheric flow sources. The main results of this study can be summarized as follows:

1. The design of an ultrasonic wind tunnel with an ejector system is possible and efficient using the steam power of the thermal power plant. There is no need to use the rotating component in the wind tunnel system, and there is no need for low-pressure and high-pressure sources in addition to power plant steam. Hence, this will significantly reduce the wind tunnel costs. Also, the existence of many combined cycle power plants in Iran and the use of a small amount of steam in the ejector wind tunnel compared to circulating steam in the power plant cycle creates a good potential for launching this project.
2. The accuracy of numerical methods is specified in ejector design. The results obtained using FLUENT software are also well consistent with previous experimental and numerical results. According to the validations performed, numerical flow simulation can be performed in the mentioned commercial software to design a wind tunnel with an ejector system.
3. The diameter of the secondary nozzle throat is a critical parameter in the design. Reducing the diameter will reduce the flow stability and oscillation of the flow characteristics in the test chamber.
4. Wind tunnel design process with an ejector system requires several stages of trial and error with a numerical method due to the nonlinear behavior of this system. The new design must be networked and simulated in the anticipated working conditions at each stage.
5. CPM method yields better results for ejector refrigeration and vacuum ejectors. However, CAM-based ejectors designed for wind tunnel

design perform better than CPM ejectors. The advantage lies in the fact that the CAM method can use a much higher entertainment ratio, which has also been noted in previous studies.

6. The most important geometric parameters in designing an ultrasonic wind tunnel with an ejector system are the area of the secondary nozzle throat and the angle of the primary divergent nozzle. These two parameters are the final determinants of the pressure behind the secondary nozzle, determining the Mach number of the wind tunnel. Due to the simultaneous effect of these two parameters on the flow behind the nozzles, the design will require trial and error.

References

[1]Hanafi, A. S., G. M. Mostafa, A. Waheed, and A. Fathy. "1-D mathematical modeling and CFD investigation on supersonic steam ejector in MED-TVC." Energy Procedia 75 (2015): 3239-3252.

[2] Nili Ahmadabadi M., Roshani, M. R., Rabiee, A. One-dimensional design of one-, two- and three-stage ultrasonic wind tunnels. Mechanics of structures and fluids. 2011 [cited 2022January16]; 1(2):57-68.

[3] Bazazzadeh, M., Dehghan Manshadi, M., Nazarian Shahrbabaki, A., Shahriari, A. Design of optimal pressure controller in a blowing ultrasonic wind tunnel using genetic algorithm. Modeling in Engineering. 2016 [cited 2022January16]; 14(47):155-169.

[4] Dolabi, H., Yousefi, A., Hashemabadi, M. Design of Supersonic Wind Tunnel Diffuser Based on Numerical Analysis of Flow Field." Amirkabir Mechanical Engineering (Amirkabir). 49.3 (2017): 457-470.

[5] Keenan, J.H, Neumann, E.P., Lustwerk, F. A simple air ejector. Journal of Applied Mechanics, Trans ASME, 1942, 64, 75–81.

[6] Keenan, J.H.; Neumann, E.P.; Lustwerk, F. An investigation of ejector design by analysis and experiment. Journal of Applied Mechanics, Trans ASME, 1950, 72, 299–309.

[7]Aidoun Z, Ameur K, Falsafioon M, Badache M. Current Advances in Ejector Modeling, Experimentation and Applications for Refrigeration and Heat Pumps. Part 1: Single-Phase Ejectors. Inventions. 2019 Mar;4(1):15.

[8] Aidoun Z, Ameur K, Falsafioon M, Badache M. Current Advances in Ejector Modeling, Experimentation and Applications for Refrigeration and Heat Pumps. Part 2: Two-Phase Ejectors. Inventions. 2019 Mar;4(1):16.

[9] Aphornratana, S.; Chungpaibulpatana, S.; Srikhirin, P. Experimental investigation of an ejector refrigerator:Effect of mixing chamber geometry on system performance. Int. J. Energy Res. 2001, 25, 397–411.

[10] Yapici, R.; Ersoy, H.K. Performance characteristics of the ejector refrigeration system based on the constantarea ejector flow model. Energy Convers. Manag. 2005, 46, 3117–3135.

[11] Pianthong, K.; Seehanam, W.; Behnia, M.; Sriveerakul, T.; Aphornratana, S. Investigation and improvement of ejector refrigeration system using computational fluid dynamics technique. Energy Convers. Manag. 2007,48, 2556–2564.

[12] Wang, J.; Tao, L.; Wang, Y.; Guo, J. CFD analysis of ejector in an ejector cooling system. In Proceedings of theInternational Congress of Refrigeration, Beijing, China, 21–26 August 2007.

[13] Sriveerakul, T.; Aphornratana, S.; Chunnanond, K. Performance prediction of steam ejector usingcomputational fluid dynamics: Part 1. Validation of the CFD results. Int. J. Therm. Sci. 2007, 46, 812–822.

[14] Varga, S.; Oliveira, A.C.; Diaconu, B. Influence of geometrical factors on steam ejector performance—A numerical assessment. Int. J. Refrig. 2009, 32, 1694–1701.

[15] Jia, Y.; Wenjian, C. Area ratio effects to the performance of air-cooled ejector refrigeration cycle with R134a refrigerant. Energy Convers. Manag. 2012, 53, 240–246.

[16] Yan, J.; Cai, W.; Lin, C.; Li, C.; Li, Y. Experimental study on performance of a hybrid ejector-vapor compression cycle. Energy Convers. Manag. 2016, 113, 36–43.

[17] Mohamed, S.; Shatilla, Y.; Zhang, T. CFD-based design and simulation of hydrocarbon ejector for cooling. Energy 2019, 167, 346–358.

[18] Pianthong, K.; Seehanam, W.; Behnia, M.; Sriveerakul, T.; Aphornratana, S. Investigation and improvement of ejector refrigeration system using computational fluid dynamics technique. Energy Convers. Manag. 2007,48, 2556–2564.

[19] Sriveerakul, T.; Aphornratana, S. Performance prediction of steam ejector using computational fluid dynamics: Part 2. Flow structure of a steam ejector influenced by operating pressures and geometries. Int. J. Therm. Sci. 2007, 46, 823–833.

[20] Huang, B.J.; Jiang, C.B.; Hu, F.L. Ejector performance characteristics and design analysis of jet refrigeration system. J. Eng. Gas. Turbine Power 1985, 107, 792–802.

[21]Ruangtrakoon, N.; Thongtip, T.; Aphornratana, S.; Sriveerakul, T. CFD simulation on the effect of primary nozzle geometries for a steam ejector in refrigeration cycle. Int. J. Therm. Sci. 2013, 63, 133–145.

[22] Riffat, S.B.; Gan, G.; Smith, S. Computational fluid dynamics applied to ejector heat pumps. Appl. Therm. Eng. 1996, 16, 291–297.

[23] Zhang, B.; Song, X.; Lv, J.; Zuo, J. Study on the key ejector structures of the waste heat-driven ejector air conditioning system with R236fa as working fluid. Energy Build. 2012, 49, 209–215.layer theory. 7th edn. McGraw-Hill, New York.